International Journal of Energy
ISSN: 2957-9473 | Vol. 3, No. 3, 2023

Experimental Study on Mechanical Characteristics of Prefabricated Fractured Sandstone Samples under Uniaxial Cyclic Compression

Dahua Ren [1, *], Chengfang Shan [3], Huiyang Shang [3], Yafeng Li [3], Wei Liu [3] and Sijiang Wei [1, 2]

[1] School of Energy Science and Engineering, Henan Polytechnic University, Jiaozuo Henan 454003, China
[2] Collaborative Innovation Center of Coal Work Safety and Clean High Efficiency Utilization, Jiaozuo, Henan 454003, China
[3] Kuqa County Yushuling Coal Mine Limited Liability Company, Kuqa City, Aksu Region, Xinjiang Uygur Autonomous Region 842000, China

*** Corresponding author:** Dahua Ren

Abstract: The loading-unloading physical and mechanical characteristics of fractured coal-bearing strata are greatly affected by fracture occurrence. In order to study the physical and mechanical response characteristics of fractured rock under cyclic compression, this paper takes prefabricated fractured sandstone samples with different dip angles as the object, and uses uniaxial cyclic loading and unloading test to study the influence of crack dip angle on sample strength, failure mode and crack propagation law. The results show that with the increase of crack inclination angle, the cyclic loading and unloading peak strength and elastic modulus of the sample increase significantly, and the peak strain decreases first and then increases. During the cyclic loading process, the area of the hysteresis loop gradually decreases, the slope gradually increases, the energy con-sumed by the hysteresis loop gradually decreases, the cumulative plastic deformation increases, and the curve shape presents a “concave” type; when it is 15 ° and 30 °, the cracks at the crack tip are wing cracks. When it is 45 °, the cracks at the crack tip are secondary inclined cracks and wing cracks. When it is 60 °, 75 ° and 90 °, the cracks at the crack tip are secondary coplanar cracks and wing cracks. With the increase of fracture dip angle, the number of cycles and peak strength at failure are increasing.

Keywords: Sandstone; Uniaxial Cyclic Loading and Unloading; Single Fracture; Peak Intensity.

1. Introduction

Coal measure rock refers to the multi-sandwich weak rock containing coal seam. Under the action of mining, blasting and impact dynamic load, joints and cracks are easy to expand and form the main control cracks, which is very important for the instability and control of surrounding rock [1]. In view of the dynamic characteristics [2], deformation characteristics and fracture propagation law of fractured rock mass [3], many scholars at home and abroad have done a lot of research. Pu et al. [4] conducted a cyclic study on the failure mode of rock materials and summarized the fracture angle at the lowest uniaxial compressive strength. In order to study the influence of joint dip angle on macro and micro fracture mechanical mechanism of three-dimensional irregular sandstone, Hao et al.[5] used RFPA3D to conduct uniaxial compression simulation of sandstone with joints with different dip angles, and revealed the influence of joint distribution and micro inhomogeneity on mechanical behavior, fracture mode and energy evolution of sandstone. Ma et al.[6] studied the deformation, strength and damage characteristics of salt rock, explored the action of cyclic load under the three-way stress state, and obtained the two-stage evolution law of axial deformation and steady-state deformation of salt rock. Zhou et al.[7] conducted uniaxial cyclic loading and unloading tests and fracture damage mechanical characterization to investigate the nature and characteristics of brittle rock. Cheng et al.[8] analyzed the evolution characteristics of absorbed dissipated energy, total energy and elastic energy during cyclic loading and unloading by means of true triaxial cyclic loading and unloading test. The results show that: the total absorbed energy, elastic energy and dissipated energy change rule has nothing to do with the crack angle of sandstone samples, and they all increase with the increase of the number of cycles, and the increase is getting bigger and bigger, and the maximum is close to the destruction. Liu et al.[9] conducted loading and unloading tests on equal amplitude cycling and step-by-step primary cycling of siltstone, and conducted an in-depth study on the evolution laws of siltstone under cyclic loading such as stress-strain curves, fracture production at the stage of destruction, and pore-fracture expansion and scale. Wang[10] studied the mechanical properties and damage characteristics of sandstone under different cyclic loading, through the comparative analysis of the stress-strain curves, peak strain, axial cumulative residual strain, axial residual strain increment and their corresponding strength and damage morphology under equal amplitude cyclic loading by using different water content, different stress amplitude, different loading rates, and combined with the SEM image to analyze the connection between the microscopic rupture characteristics of the sandstone and the macroscopic fracture damage, so as to discuss the evolution law of the rocks under the action of cyclic loading from the microscopic point of view. He[11] studied the strain development near the crack of the rock sample by attaching strain gauge to the tip of the prefabricated crack samples, and concluded that the axial strain gradually increased with the increase of the crack angle during the failure of the rock samples. At present, although certain research results have been achieved in the field of cyclic loading and unloading, there are still relatively many researches on uniaxial loading and unloading, while relatively few researches on triaxial loading and unloading test. In terms of cyclic loading and unloading test, there are few relevant researches on rocks containing cracks. Now, uniaxial cyclic

loading and unloading tests are carried out on sandstone samples containing prefabricated cracks to systematically analyze the influence of crack inclination on the strength, deformation characteristics and crack extension law of fractured rocks by changing the crack inclination of prefabricated cracks.

2. Overview of the Experiment

2.1. Test Materials and Sample Preparation

The sandstone extracted from the excavation head of 1605 intermediate bottom pumping lane of Guhanshan Mine of Henan Coking Coal Energy Company Limited was used as the research object, and there were no obvious macro-cracks and man-made damages on the rock samples from the external view. All sandstone samples were taken from the same sandstone block, processed into 50mm×100mm standard samples, and the non-parallelism and non-perpendicularity of the two end surfaces were not more than 0.02 mm.

As shown in Figure 1(a), cracks were pre-arranged in the central position of the side of the sample, and strain gauges were pasted on both ends of the cracks. The angles between the cracks and the end face were 15°, 30°, 45°, 60°, 75° and 90°, with one sample in each group, and the crack length was 2a=20mm. The prefabricated crack sample is shown in Figure 1(b).

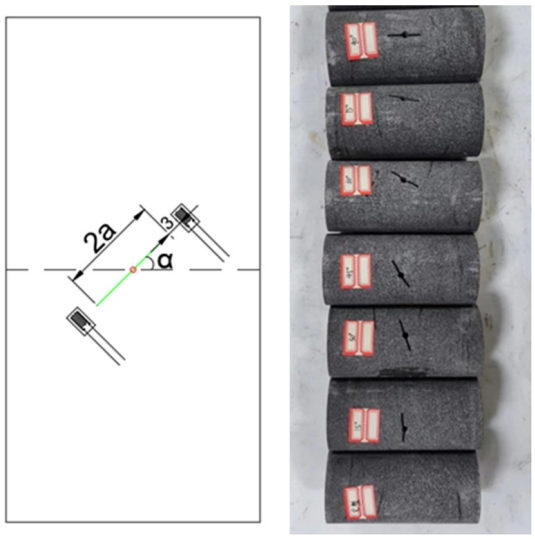

(a) (b)

Fig 1. Schematic diagram of geometric parameters of pre-cast crack and sandstone sample

The size, mass and wave velocity of prefabricated fractured sandstone were measured, and the density of each sample was calculated to obtain the physical parameters of each group of samples, as shown in Table 1. It can be seen that the mass of sandstone samples used in this experiment ranged from 497.38 to 503.89g, with an average value of 499.56g. The height is 99.74~100.11mm, the average is 99.93mm; The diameter was 49.51~49.71mm, and the mean value was 49.62mm. The apparent density ranged from 2.580 to 2.603 g/cm3, with an average of 2.586 g/cm3. When the wave velocity of the sample is measured, each sample is measured three times, and the average value is taken as the wave velocity of the sample. The wave velocity of the sandstone sample is 3.677~3.846 km/s, and the average value is 3.729km/s.

As can be seen from Table 1, the quality and size of the sandstone samples used in this test are relatively similar, with good homogeneity and little difference in density, indicating that the samples suffered less external damage during transportation. At the same time, it is also found that there are certain differences in the wave velocity of the samples. The wave velocity of the complete samples is slightly higher than that of the prefabricated crack samples, but the wave velocity of the prefabricated crack samples is close to that of the prefabricated crack samples. When ultrasonic waves pass through these cracks, they will appear refraction, reflection and other forms of reflection, resulting in lower longitudinal wave velocity of prefabricated crack samples.

Table 1. Physical parameters of the sample

serial number	quality/g	h/mm	d/mm	ρ (g/cm^3)	wave velocity (km/s)
complete	503.89	99.76	49.71	2.603	3.846
15°	498.13	100.06	49.57	2.580	3.694
30°	499.49	99.74	49.58	2.594	3.713
45°	499.99	99.92	49.69	2.580	3.731
60°	498.21	99.91	49.64	2.577	3.677
75°	499.84	99.99	49.51	2.597	3.750
90°	497.38	100.11	49.62	2.569	3.694

2.2. Test Loading Program and Data Acquisition

The test system is composed of loading and strain collection, which can monitor and record the stress, strain and crack tip strain information of the sample during cyclic loading and unloading. The instrument used in the loading system is RMT-150B type electro-hydraulic servo rock mechanics testing machine, which has two control systems: displacement control and load control.

The strain gauge is pasted at 2mm of the precast crack tip. The strain gauge is at an angle of 90° from the crack direction. The strain gauge is pasted at both ends of the crack. First, the surface of the prefabricated crack sample is polished with sandpaper, and then the surface of the sample is wiped with medical alcohol. A and B adhesive are used between the strain gauge and the sample. Finally, the strain collection system is connected with a wire, and the system automatically records the strain collection data of the crack tip. The 12-channel XL210C program-controlled static resistance strain gauge was used in this experiment.

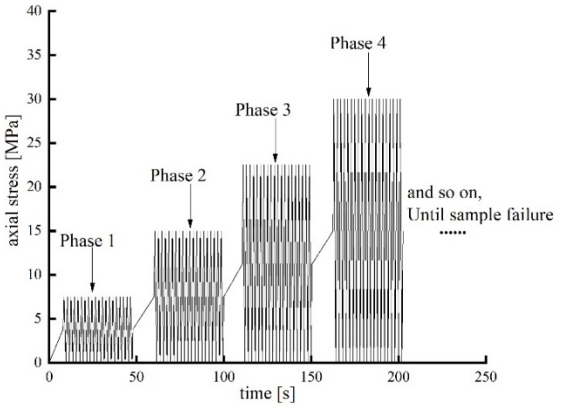

Fig 2. Stress and time curve

In this test, the loading and unloading rate is set at 100N/s by means of load control. Uniaxial compression and cyclic loading and unloading experiments are carried out. During cyclic loading and unloading, the lower limit of stress is kept

unchanged (the lower limit of stress is 0), the upper limit of stress is increased by 7.5MPa each time, and the cycle is 20 times in each stage (0-7.5MPa, 0-15MPa, 0-22.5MPa, ...). The relationship curve between stress and time during loading and unloading of the sample is shown in Figure 2.

3. Test Results and Analysis

3.1. Uniaxial Compression Test of Crack Sample

Uniaxial compression test was carried out on sandstone samples, the loading control mode was selected, the loading rate was 100N/s, and the elastic modulus, peak strain, peak stress and other parameters of sandstone samples were recorded.

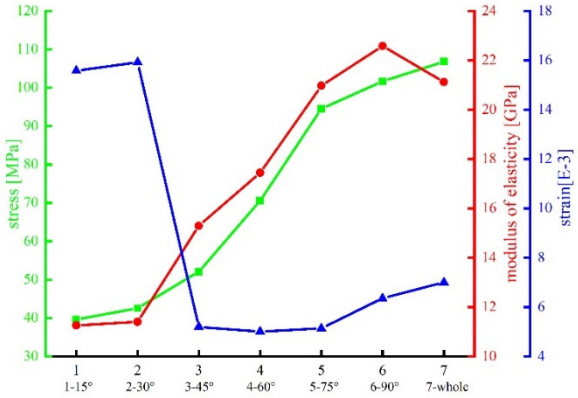

Fig 3. Comparison of peak stress, elastic modulus and strain at different crack inclination angles

According to Figure. 3, with the increase of crack angle, the cyclic loading and unloading strength of the sample shows a gradual upward trend, and the highest uniaxial compressive strength of the sample with crack reaches 101.60MPa, which is 95.1% of that of the complete sample. The lowest compressive strength is 39.60MPa, which is 37.1% of the complete sample. When the crack dip is 15° and 30°, the samples are mainly subjected to compression failure, and there is little difference in cyclic loading and unloading strength. When the crack angle is 45°~90°, the shear failure of the sample is the main one, and the cyclic loading and unloading strength of the sample increases significantly. With the increase of the crack inclination angle, the vertical projection area of the crack decreases gradually, and the area resisting uniaxial compression increases gradually. Therefore, with the increase of the crack inclination angle, the cyclic loading and unloading strength of the sample shows a trend of gradual increase, and the penetration of a single crack has a significant impact on the strength of the sample. The elastic modulus increases gradually with the increase of crack angle, which is consistent with the increase of peak stress. The strain of the sample reaches the maximum when the crack dip is 15° and 30°, because in the process of cyclic loading and unloading, the crack is gradually compacted, and the upper part of the crack occurs a small displacement directly downwards, making the overall displacement larger than that of other crack inclination samples. Therefore, the peak strain reaches the maximum when the crack dip is 15° and 30°.

3.2. Stress-strain Curve Analysis of Sandstone with Prefabricated Cracks

Stress-strain curves and local enlargements of the first stage of pre-cycling for sandstone samples containing prefabricated cracks with 90° inclination dip are given in Figure. 4.

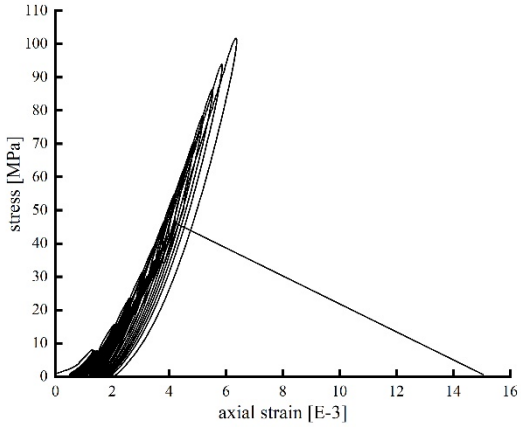

(a) Full-cycle uniaxial loading and unloading stress-strain

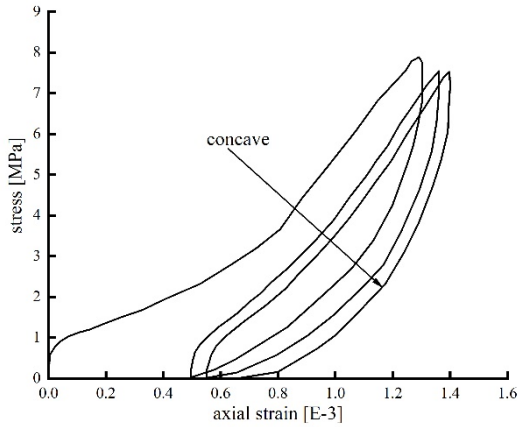

(b) Stress-strain curves curve for the phase 1 of pre-cycling

Fig 4. Stress-strain curve of 90° precast fractured sandstone under uniaxial cyclic loading and unloading

As can be seen from Figure. 4 (a), in the early loading stage of the sample, the sandstone containing prefabricated cracks showed significant nonlinear changes, mainly because the sandstone sample contained a large number of internal damage such as micro-cracks and holes. After loading, the sample was continuously compacted or closed due to a large number of internal damage such as micro-cracks in the sandstone, and the bearing capacity of the sample gradually increased. The tangential modulus also increases. With the increase of axial stress, the rock samples gradually enter the stage of cyclic loading and unloading. As can be seen from Figure. 4 (b), the cyclic loading and unloading curves at all levels are of the “concave” type, and the loading and unloading paths of the curves do not overlap with each other, constituting a plastic hysteresis loop; with the continuous loading, the area of the hysteresis loop decreases gradually, and the energy consumed decreases from one level to another, and the cumulative plastic deformation of the sample increases.

In the early stage of loading, the micro-cracks are gradually squeezed and compacted, and the bearing capacity of the sample is enhanced, which is reflected in the increase of the slope of the stress-strain curve. During unloading, as the axial stress decreases, the tiny cracks and pores that were previously compacted gradually recover, so that the slope of the curve becomes smaller and smaller, so the cyclic loading and unloading curve will be “concave”.

3.3. Sample Deformation Characteristic

3.3.1. Distribution of Major Cracks at the Tip of the Prefabricated Slit

At present, many scholars at home and abroad have done a lot of research on the initiation mechanism of prefabricated crack tip micro-cracks [12-15], and the results have been widely accepted. It was found that the crack distribution at the prefabricated crack tip was dominated by wing crack, followed by secondary inclined crack and secondary coplanar crack, as shown in Figure. 5.

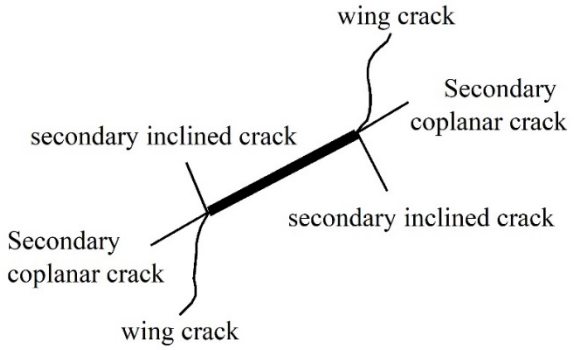

Fig 5. Distribution diagram of the main cracks at the precast crack tip

(1) Wing crack: the wing crack extends from the crack tip in a curvilinear path, eventually tends to expand in the direction of the maximum principal stress, and steadily expands with the increase of load.

(2) Secondary inclined crack: The secondary inclined crack is perpendicular to the prefabricated crack, the expansion rate is slow, and the secondary inclined crack rarely appears in the failure process of the sample.

(3) Secondary coplanar crack: spread along the prefabricated crack, when the secondary coplanar crack occurs, the crack penetration speed becomes faster, there is a thin sheet material on the crack surface and formed along the crack surface.

3.3.2. Influence of Crack Angle on Crack Penetration Patterns in Rock Samples

Figure. 6 shows the final failure mode and its sketch of each group of samples under cyclic loading and unloading. In this cyclic experiment, micro-cracks appear in the crack tips of each sample, indicating that stress concentration occurs in the precast crack tips under cyclic loading and unloading. Further analysis of crack propagation showed that different degrees of crack penetration occurred in all samples.

Figure. 7 shows the change of strain at crack tip with loading and unloading time and the total number of stages of cyclic loading and unloading of samples at different inclination angles. It can be seen that different fracture inclination angles have different failure modes during loading and unloading. When the fracture inclination is 15°, the sample will fail in the second cycle stage, and then with the increase of the fracture inclination, the sample will fail in the 6th, 7th, 9th, 12th and 13th cycle stages respectively. It can be found that the number of cyclic loading and unloading of the sample is closely related to the dip angle of the fracture. With the increase of the dip angle, the number of cycle stages increases gradually, and the peak strength of the sample is also gradually enhanced.

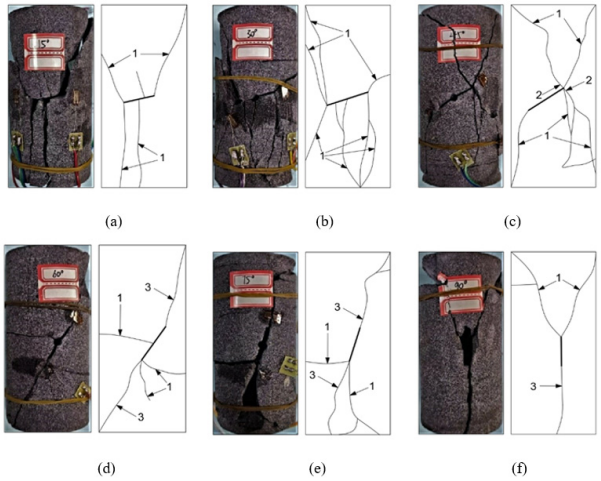

(1- wing crack; 2- secondary inclined crack; 3-secondary coplanar crack)

Fig 6. Failure modes and sketches of samples with different fracture dip angles

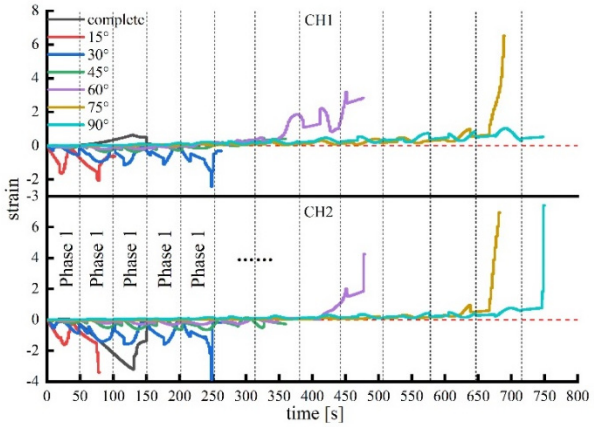

Fig 7. Strain-time curve of crack tip

As can be seen from Figure. 6 and Figure. 7, when α is 15° and 30°, the crack at the crack tip is the wing crack. With the continuous increase of axial stress, the crack expands in the direction of the maximum principal stress and finally penetrates the sample. Through the observation of the fracture surface, it is found that the particles on the fracture surface have wear marks. Therefore, it can be concluded that there is shear stress on the micro-crack surface at the crack tip when the crack inclination is 15° and 30°, but the tensile stress plays a major role in the crack propagation. When α is 45°, the cracks at the crack tip are wing cracks and secondary inclined cracks. With the continuous expansion of cracks, the mixed lap phenomenon of wing cracks and secondary inclined cracks occurs, and the sample is finally penetrated. However, the co-existence of wing cracks and secondary inclined cracks occurs only at the upper crack tip, while only wing cracks occur at the lower tip. The author believes that this phenomenon may be caused by the delay of stress transfer during cyclic loading. When α is 60°, 75°, 90°, the cracks at the crack tip are wing cracks and secondary coplanar cracks. With the process of cyclic loading and unloading, the cracks finally penetrate the sample. When α is 60° and 75°, secondary coplanar cracks are generated in both the upper and lower tips and penetrate the sample, and a horizontal wing crack is generated in both of them. When α is 90°, only a secondary coplanar crack occurs at the lower tip of the sample and penetrates through the sample, and a "V" wing crack occurs at the initiation of the upper tip. In general, when α is

90°, the wing crack and secondary coplanar crack together form a “Y” type crack and penetrate the sample in a “Y” shape. It can be seen that the crack inclination angle has a great influence on the crack initiation and penetration mode of rock samples.

4. Conclusion

Uniaxial cyclic loading and unloading tests were carried out on sandstone samples with different crack inclination angles to study the effects of crack inclination angle on sample strength, fracture mode and crack growth rule under cyclic load. It is found that:

(1) With the increase of crack inclination angle, the peak strength and elastic modulus of the sample during cyclic loading and unloading increase significantly, and the peak strain decreases first and then increases, reaching the maximum at 15° and 30°.

(2) In the early stage of sample loading, sandstone containing prefabricated cracks presents significant nonlinear changes. With the continuous loading, the area of hysteresis loop gradually decreases, the energy consumed gradually decreases, the cumulative plastic deformation of the sample gradually increases, and the cyclic loading and unloading curves at all levels are “concave”.

(3) The Times of cyclic loading and unloading of the sample are closely related to the inclination angle of the fracture. With the increase of the inclination angle, the number of cyclic stages increases gradually, and the peak strength of the sample also increases gradually.

(4) When α is 15° and 30°, the crack at the crack tip is wing crack, and the penetration mode is mainly tensile penetration; when α is 45°, the crack at the crack tip is secondary inclined crack and wing crack, and the penetration mode is tensile shear penetration; when α is 60°, 75° and 90°, the crack at the crack tip is secondary inclined crack and wing crack, and the penetration mode is tensile shear penetration. The cracks at the crack tip are secondary coplanar cracks and wing cracks, which are mainly tensile shear penetrating.

Acknowledgments

This work was supported in part by the National Natural Science Foundation of China under grants (52174074) and Supported by Program for Innovative Research Team (in Science and Technology) in University of Henan Province (22IRTSTHN005); Open Fund of Key Laboratory of Efficient Mining and Comprehensive Utilization of Mineral Resources in Henan Province (KCF2205).

References

[1] MS Gao, YM Liu, YC Zhao, et al. Roof burst in-stability mechanism and dynamic characteristic of deep coal roadway subjected to rock burst. Journal of China Coal Society, 2017, 42 (7): 1650−1655 (in Chinese).

[2] ZH Jiao, YD Jiang, YX Zhao, et al. Energy dissi-pation and damage characteristics of lateral-restraintcoal un-der impactload. Journal of China University of Min-ing& Technology, 2023, 52 (3): 492-501. (in Chinese).

[3] JG Wang, YH Guo, XH Zhang, et al. Me-chanics properties of simulated rock affected by layer joints under impact loading. Chinese Journal of Underground Space and Engineering, 2017, 13 (S2): 559-564. (in Chinese).

[4] CZ Pu, P Cao, YL Zhao, et al. Numerical analy-sis and strength experiment of rock-like materials with mul-ti-fissures under uniaxial compression. Rock and Soil Me-chanics, 2010, 31 (11): 3661-3666. (in Chinese).

[5] ZB Hao, YJ Zuo, H Liu, et al. Study on the influ-ence of joint dip angle on the fracture mechanical mecha-nism of irregular sandstone. Chinese Journal of Under-ground Space and Engineering, 2022, 18 (06): 1906-1915. (in Chinese).

[6] JL Ma, XY Liu, HF Xu, et al. Experimental study on triaxial deformation and strength characteristics of salt rock under cyclic loading. Chinese Journal of Rock Me-chanics and Engineering, 2013, 32 (04): 849-856. (in Chi-nese).

[7] JW Zhou, GX Yang, WX Fu, et al. Study on uni-axial cyclic loading and unloading test and fracture damage mechanical properties of brittle rock. Chinese Journal of Rock Mechanics and Engineering, 2010, 29 (06): 1172-1183. (in Chinese).

[8] J Cheng, CQ Liu. Study on energy evolution law of fractured sandstone under true triaxial loading and unloading. Chinese Journal of Underground Space and Engineering, 2023, 19 (01): 117-125. (in Chinese).

[9] XY Liu, ZY Chai, X Liu, et al. Characteristics of pore crack propagation and unloading failure of siltstone under cyclic loading. Journal of China Coal Society, 2022, 47 (S1): 77-89. (in Chinese).

[10] H Wang. Study on mechanical properties and damage characteristics of sandstone under different cyclic loads. (MS., Anhui University of Science and Technology, China, 2021).

[11] T He. Experimental study on the influence of prefabricat-ed cracks on the mechanical properties of granite. (MS., Hubei University of Technology, China, 2021).

[12] P Zhang, N Li, RL He. Study on localized progres-sive damage model of fractured rock-like materials. Chi-nese Journal of Rock Mechanics and Engineering, 200(10): 2043-2050. (in Chinese).

[13] P Zhang. Study on failure mode and localized progressive failure model of fractured media under static and dynamic stress conditions. Chinese Journal of Rock Mechanics and Engineering, 2005 (15): 2802. (in Chinese).

[14] ML Huang, KZ Huang. Experimental study on propa-gation mechanism of three-dimensional surface crack inter-action. Chinese Journal of Rock Mechanics and Engi-neering, 2007, No.188 (09): 1794-1799. (in Chinese).

[15] KZ Huang, P Lin, CA Tang, et al. Study on the coalescence mechanism of intermittent preset cracks under biaxial loading. Chinese Journal of Rock Mechanics and Engineering, 2002 (06): 808-816. (in Chinese).